Calorimetric studies on the influence of *N*-methylated headgroups on the mixing behavior of diheptadecanoyl phosphatidylcholine with 1-behenoyl-2-lauroylphosphatidylcholine

Robert B. Sisk and Ching-hsien Huang
Department of Biochemistry, Health Sciences Center, University of Virginia, Charlottesville, Virginia 22908 USA

ABSTRACT Recent studies of five different phosphatidylcholine/phosphatidylcholine (PC/PC) systems indicate that binary mixtures of phosphatidylcholines in which one component has a normalized chain length difference (ΔC/CL) in the range of 0.09–0.40 and the other a ΔC/CL in the range of 0.42–0.57 exhibit the phase behavior of a eutectic system. Here, ΔC is the effective chain-length difference between the two acyl chains, and CL is the effective length of the longer of the two acyl chains for the same lipid molecule in the gel state. In each mixture, gel phase immiscibility occurs over a wide compositional range due to the difference in the gel phase acyl chain packing properties of each component. Although the mixtures differ in the location of their eutectic horizontal, with respect to temperature, all have a similar eutectic point that occurs at a composition of ~40 mol percent of the component with the ΔC/CL value in the range of 0.42–0.57. Here, we extend these studies by systematically modifying the headgroup of C(17):C(17)PC and then analyzing the mixing behavior of the modified lipid with C(22):C(12)PC using DSC. Progressive demethylation of the C(17):C(17)PC headgroup leads to an increase in gel phase immiscibility and a decrease in the amount of C(22):C(12)PC that comprises the eutectic composition. The temperature defining the location of the eutectic horizontal, however, remains virtually unchanged in all three phase diagrams. Our results suggest that the eutectic composition is influenced by changes in gel phase acyl chain packing that are dependent on headgroup–headgroup interactions. In contrast, the eutectic nature of the phase diagram and the location of its solidus line are properties of acyl chain interactions that are independent of phospholipid headgroup–headgroup interactions.

INTRODUCTION

Biological membranes are well known to contain lipid bilayers composed principally of phospholipid molecules that have asymmetrical acyl chains with respect to chain length. The normalized chain-length difference between the *sn*-1 and *sn*-2 acyl chains for a phosphatidylcholine molecule in the gel state is represented by the structural parameter, ΔC/CL (Mason et al., 1981*b*; Huang, 1991). ΔC is the effective chain-length difference, in C–C bonds, between the two acyl chains and CL is the effective length of the longer of the two acyl chains, in C–C bonds. Conformational disparity between the *sn*-1 and *sn*-2 acyl chains appears to be a fundamental feature for phosphatidylcholines in the gel state bilayer (Yeagle, 1987). In calculating values of ΔC and CL, the inherent shortening of 1.5 C–C bond lengths for the *sn*-2 acyl chain is accounted for.

Recently, the effect of phospholipid acyl chain-length difference between the *sn*-1 and *sn*-2 acyl chains on the thermotropic phase behavior of the aqueous lipid dispersion has been studied extensively by high-resolution differential scanning calorimetry (DSC) for four series of mixed-chain phosphatidylcholines with respective molecular weights (MW) identical to those of C(17):C(17)PC (Huang, 1990; Lin et al., 1990), C(16):C(16)PC (Bultmann et al., 1991), C(15):C(15)PC, and C(14):C(14)PC (Lin et al., 1991). These studies show that the thermodynamic parameters associated with the main phase transitions (T_m, ΔH, and ΔS) of these lipid dispersions exhibit a biphasic behavior when plotted as a function of ΔC/CL, with a breakpoint occurring at a ΔC/CL value of ~0.42. Phospholipids with ΔC/CL values considerably lower than 0.42 have been shown to self-assemble, in excess water, into a partially interdigitated type of gel phase packing motif in which the *sn*-1 acyl chain of one phospholipid packs end to end with the *sn*-2 acyl chain of another phospholipid from the opposing leaflet, at $T < T_m$ (Slater and Huang, 1988). As the ΔC/CL value increases, this type of packing motif continuously displaces the bulky terminal methyl groups of the two acyl chains packed end to end away from the center of the bilayer towards the interfacial region (Sisk et al., 1990). As the displacement increases, the perturbation of adjacent acyl chains also increases until a point is reached where it becomes energetically more favorable to convert to an alternative packing motif. This point, represented by a ΔC/CL value of ~0.42, is where the phospholipid packing motif changes from a partially interdigitated to a mixed interdigitated type.

There is a significant difference in gel phase bilayer

Address correspondence to Dr. Huang.

0006-3495/92/03/593/11 $2.00

thickness between a partially interdigitated and a mixed interdigitated bilayer (McIntosh et al., 1984; Hui et al., 1984; Mattai et al., 1987; Shah et al., 1990). This is consistent with the mixing behavior of binary lipid mixtures as demonstrated by DSC studies on binary mixtures composed of identical MW phosphatidylcholines in which one phospholipid has a ΔC/CL value below, and the other a value above, 0.42 (Lin and Huang, 1988; Sisk et al. 1990; Bultmann et al., 1991). C(17):C(17)PC is an identical-chain phospholipid with a MW of 762.2 and a ΔC/CL value of 0.094. Because acyl chain bending shortens the *sn*-2 chain by 1.5 C–C bond lengths, C(17):C(17)PC gel phase bilayers are slightly interdigitated at $T < T_m$. The main phase transition for pure C(17):C(17)PC bilayers is the $P_{\beta'}$ to L_α phase transition, where $P_{\beta'}$ is the periodic ripple phase and L_α is the liquid-crystalline or fluid phase. C(22):C(12)PC is equal in MW to C(17):C(17)PC, but has a ΔC/CL value of 0.548. As a result of its highly asymmetric acyl chains, the C(22):C(12)PC bilayer undergoes a main phase transition upon heating that corresponds to the melting of the mixed-interdigitated gel into a partially interdigitated (L_α) fluid phase. Because of different gel phase packing motifs, C(17):C(17)PC bilayers are thicker than C(22):C(12)PC bilayers at $T < T_m$. However, L_α phase bilayers for both lipids are about equal in thickness as a result of *trans*-gauche isomerizations of the methylene units in the acyl chains and the change in chain packing motif for C(22):C(12)PC bilayers at $T > T_m$. The temperature-composition phase diagram for binary mixtures of C(22):C(12)PC/C(17):C(17)PC indicates large areas of both gel phase immiscibility and L_α phase miscibility in support of this analysis (Sisk et al., 1990). Because both lipid components have the same type of headgroup, phosphorylcholine, their degree of mixing is regulated primarily by differences in the hydrocarbon regions of the component lipids.

Five PC/PC eutectic phase diagrams have been published to date where the ΔC/CL value of one phosphatidylcholine component is <0.42 and the other is above 0.42: C(16):C(16)PC/C(10):C(22)PC (Bultmann et al., 1991), C(14):C(14)PC/C(18):C(10)PC (Lin and Huang, 1988), C(16):C(16)PC/C(12):C(24)PC (Gardam and Silvius, 1989), C(22):C(12)PC/C(17):C(17)PC and C(22):C(12)PC/C(15):C(19)PC (Sisk et al., 1990). All five of these phase diagrams have eutectic points located at a composition of ~40 mol percent of the higher melting lipid component. The temperature component of the eutectic horizontal, however, varies with the combination of phospholipids.

It is generally known that addition of phosphatidylethanolamine to a phosphatidylcholine bilayer increases lateral separation of the two components in the plane of the bilayer (Silvius, 1986). Because the eutectic phase diagram of C(22):C(12)PC/C(17):C(17)PC is well characterized, we can systematically modify the headgroup of C(17):C(17)PC and then analyze the mixing behavior of the modified lipids with C(22):C(12)PC. By comparing these phase diagrams with the phase diagram of C(22):C(12)PC/C(17):C(17)PC, we can assess the importance of the headgroup in the lipid–lipid interactions in the two-dimensional plane of the lipid bilayer. Note that headgroup modifications do not effect the ΔC/CL value of a phospholipid. In the present work we have investigated the binary mixing behavior of C(22):C(12)PC with C(17):C(17)PX, where PX represents the headgroups *N,N*-dimethyl-ethanolamine, *N*-methyl-ethanolamine, and ethanolamine.

MATERIALS AND METHODS

Synthetic diheptadecanoyl- and monobehenoyl phosphatidylcholine of purity greater than 99% were purchased from Avanti Polar Lipids, Inc., (Alabaster, AL). Ethanolamine hydrochloride of purity >99% was obtained from Aldrich Chemical Co. (Milwaukee, WI). Phospholipase D, type I from cabbage, and lauric anhydride were purchased from Sigma Chemical Co. (St. Louis, MO). Gaseous HCl was obtained from Matheson Gas Products (East Rutherford, NJ). Absolute ether with a trace of alcohol was purchased from EM Science (Gibbstown, NJ); this chemical was further purified by column chromatography on activated alumina to remove the alcohol before use (Perrin and Armarego, 1988). HPLC grade chloroform was purchased from J. T. Baker Chemical Co. (Phillipsburg, NJ) and further purified by refluxing with P_2O_5 and distilling. Other reagents and organic solvents were of spectral grade or the highest available purity.

Crystalline *N*-methylethanolamine hydrochloride and *N,N*-dimethylethanolamine hydrochloride were prepared as described by Gagne et al. (1985). Diheptadecanoylphosphatidyl-*N*-methyl- (*N*-methyl-C(17):C(17)PE), diheptadecanoylphosphatidyl-*N,N*-dimethyl- (*N,N*-dimethyl-C(17):C(17)PE), and diheptadecanoylphosphatidylethanolamine (C(17):C(17)PE) was synthesized by base exchange transphosphatidylation from C(17):C(17)PC using phospholipase *D* in the presence of excess *N*-methylethanolamine, *N,N*-dimethylethanolamine, or ethanolamine hydrochloride respectively (Comfurius and Zwaal, 1977). C(22):C(12)PC was synthesized by reacylation of monobehenoyl phosphatidylcholine with lauric anhydride at room temperature. The reacylation was catalyzed by 4-pyrrolidinopyridine in dry chloroform and the product was purified by silicic acid column chromatography employing a gradient of chloroform and methanol as described elsewhere (Mason et al., 1981*a*).

The method of Lin and Huang (1988) was used to produce liposomes containing a mixture of C(22):C(12)PC and either C(17):C(17)PC, *N*-methyl-C(17):C(17)PE, *N,N*-dimethyl-C(17):C(17)PE, or C(17):C(17)PE. Dried powders of preweighed C(22):C(12)PC and the corresponding C(17):C(17)PX were dissolved in $CHCl_3$. After thoroughly vortexing, the solvent was removed by a stream of N_2 gas. The dried film of the lipid mixture was resuspended in benzene and then colyophilized. The lyophilized mixture was dispersed in a NaCl (25 mM) aqueous solution containing 5 mM phosphate buffer and 1 mM EDTA (pH 7.4) to give a final lipid concentration of 5–6 mM. Samples were stored at 0°C for a minimum of 24 h before scanning. All samples were scanned at least three times in the heating direction within the range shown in the figure for a given sample.

DSC experiments were performed using a high-resolution MC-2 differential scanning calorimeter equipped with the DA-2 digital

interface and data acquisition utility for automatic collection (Microcal Inc., Northampton, MA) or a Hart 7708 differential scanning calorimeter (Hart Scientific, Pleasant Grove, UT). In all experiments, a constant heating scan rate of 15°C/h was used and samples were scanned a minimum of three times with at least 60–90 min of equilibration at low temperatures between scans. Transition temperatures (T_m) were taken from the transition peaks at the maximum peak height positions, and calorimetric enthalpies (ΔH) were calculated from the peak areas using software provided by Microcal or Hart Inc. The onset and completion temperatures of the thermal transition were extrapolated from the intercepts of maximal slopes of the onset and completion boundaries, respectively, of the transition curve with the baseline. Phase diagrams were constructed after correcting the onset and completion temperatures for the finite transition widths of the pure components (Mabrey and Sturtevant, 1976). The corrected onset and completion temperatures of the various transition curves are plotted with respect to composition of the higher melting component. The plot of onset temperatures vs mol percent composition forms the solidus line of the phase diagram (the line in Fig. 3 that separates the G_1, $G_1 + G_2$, and G_2 regions from the $L + G_1$ and $L + G_2$ regions) and the plot of completion temperatures vs mole percent forms the liquidous line of the phase diagram (the line in Fig. 3 that separates the $L + G_1$ and $L + G_2$ regions from the L region). For example, in Fig. 2, the DSC scan for 20 mol % C(17):C(17)PE$(CH_3)_2$ has a corrected onset and a corrected completion temperature of 37.7 and 41.62°C, respectively. When 37.7°C is plotted with respect to the 20 mol % concentration of C(17):C(17)PE$(CH_3)_2$ it makes a point on the solidus line (Fig. 3). When the 41.62°C is plotted with respect to the 20 mol % concentration of C(17):C(17)PE$(CH_3)_2$ it forms a point on the liquidous line (Fig. 3). At least four DSC heating scans were collected for all samples containing either *N,N*-dimethyl-C(17):C(17)PE, *N*-methyl-C(17):C(17)PE, or C(17):C(17)PE. This was done to ensure complete hydration of the sample. Because the T_m for these samples did not change significantly after the first DSC heating scan we concluded that all subsequent scans reflect the fully hydrated bilayer. The phase diagrams were constructed using values from the third DSC heating scans.

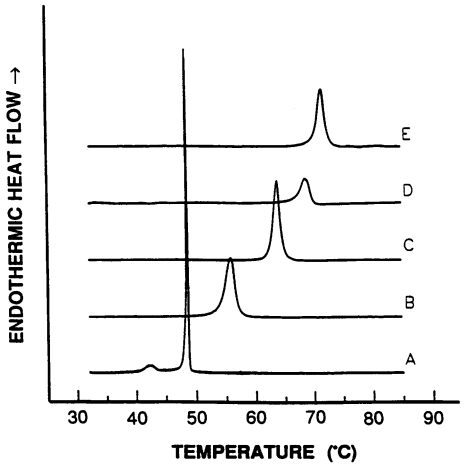

FIGURE 1 Typical DSC heating thermograms for: C(17):C(17)PC (*A*), C(17):C(17)PE$(CH_3)_2$ (*B*), C(17):C(17)PE(CH_3) (*C*), C(17):C(17)PE second heating scan (*D*), and C(17):C(17)PE first heating scan (*E*).

RESULTS

Binary mixtures of C(22):C(12)PC/*N,N*-dimethyl-C(17):C(17)PE

The mixing behavior as a function of temperature was investigated calorimetrically for a series of C(22):C(12)PC/*N,N*-dimethyl-C(17):C(17)PE samples with increasing mole percent *N,N*-dimethyl-C(17):C(17)PE. Aqueous dispersions of the pure phospholipid *N,N*-dimethyl-C(17):C(17)PE display a single endothermic transition with a T_m at 55.6 ± 0.2°C and a transition enthalpy of 11.7 kcal/mol (Fig. 1 *B*). The third DSC scans of C(22):C(12)PC/*N,N*-dimethyl-C(17):C(17)PE mixtures with various molar ratios, after samples have been scanned twice from 25 to 68°C to ensure identical

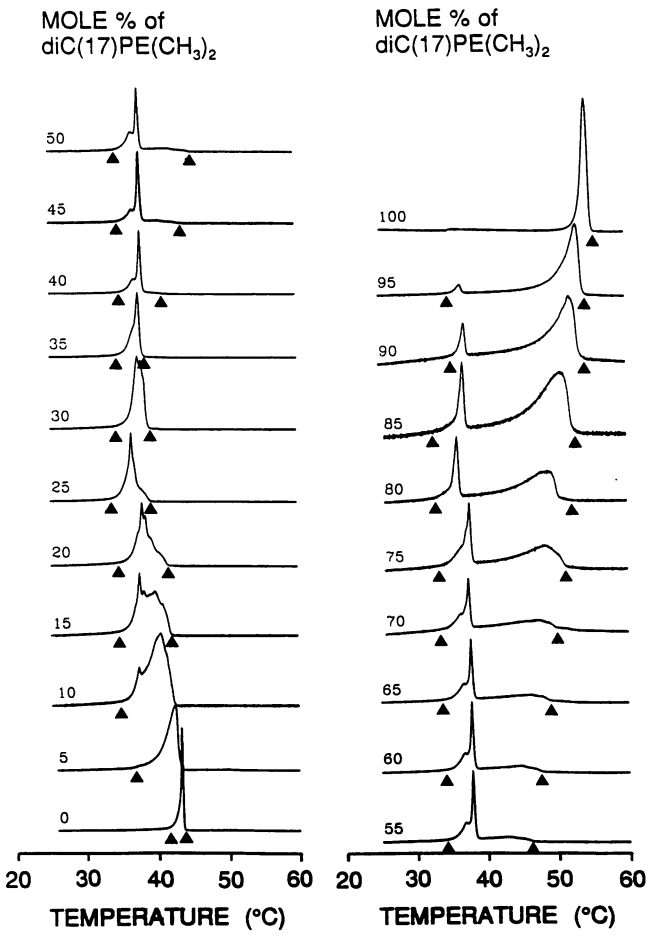

FIGURE 2 DSC heating thermograms for aqueous dispersions of C(22):C(12)PC containing various amounts of C(17):C(17)PE$(CH_3)_2$. The mole percent of C(17):C(17)PE$(CH_3)_2$ in each of the binary mixtures is indicated adjacent to the respective thermogram. The onset and completion temperatures of the main transitions are indicated by the triangles.

thermal history, are shown in Fig. 2. As the mol percent of *N,N*-dimethyl-C(17):C(17)PE incorporated into C(22):C(12)PC bilayers increases, the transition temperature of the mixture decreases from 43.1 ± 0.5°C (100 mol % C(22):C(12)PC) to 37.9 ± 0.5°C (35 mol percent *N,N*-dimethyl-C(17):C(17)PE) and then increases continuously up to 55.6 ± 0.2°C (100 mol % *N,N*-dimethyl-C(17):C(17)PE). Incorporation of 5–10 mol % *N,N*-dimethyl-C(17):C(17)PE broadens the single transition DSC curves shown in Fig. 2. Increasing the *N,N*-dimethyl-C(17):C(17)PE content to 35 mol % progressively narrows the transition. At 35 mol % *N,N*-dimethyl-C(17):C(17)PE, the transition curve is the sharpest of all DSC curves obtained for the C(22):C(12)PC/*N,N*-dimethyl-C(17):C(17)PE mixtures. Above 35 mol % *N,N*-dimethyl-C(17):C(17)PE, the transition curves gradually broaden up to ~85 mol % *N,N*-dimethyl-C(17):C(17)PE and then narrow up to the composition reaches 100 mol percent *N,N*-dimethyl-C(17):C(17)PE.

A temperature-composition phase diagram for C(22):C(12)PC/*N,N*-dimethyl-C(17):C(17)PE mixtures Fig. 3 was constructed based on the onset and completion temperatures of the transition curves as indicated by the triangles in Fig. 2. This eutectic phase diagram is similar to the one for binary mixtures of C(22):C(12)PC/C(17):C(17)PC (Sisk et al., 1990). In Fig. 3 the eutectic horizontal is located at about 37.9 ± 0.5°C and extends from roughly 8–85 mol % *N,N*-dimethyl-C(17):C(17)PE. The eutectic point occurs at 33 mol % *N,N*-dimethyl-C(17):C(17)PE and 37.9 ± 0.5°C.

Binary mixtures of C(22):C(12)PC/*N*-methyl-C(17):C(17)PE

After examining the mixing behavior of C(22):C(12)PC/*N,N*-dimethyl-C(17):C(17)PE mixtures, the role of the polar headgroup of C(17):C(17)PC in the mixing behavior of C(22):C(12)PC/C(17):C(17)PC binary mixtures was further investigated by DSC studies of C(22):C(12)PC/*N*-methyl-C(17):C(17)PE mixtures. DSC scans of aqueous dispersions of pure *N*-methyl-C(17):C(17)PE display a single transition with a T_m of 63.6 ± 0.25°C and an enthalpy of 10.7 kcal/mol (Fig. 1 *C*). Fig. 4 depicts typical DSC heating thermograms for aqueous dispersions of C(22):C(12)PC/*N*-methyl-C(17):C(17)PE binary mixtures. These thermograms represent the third DSC heating scans for each sample. All samples were scanned over the temperature range of 25 to 68°C. As

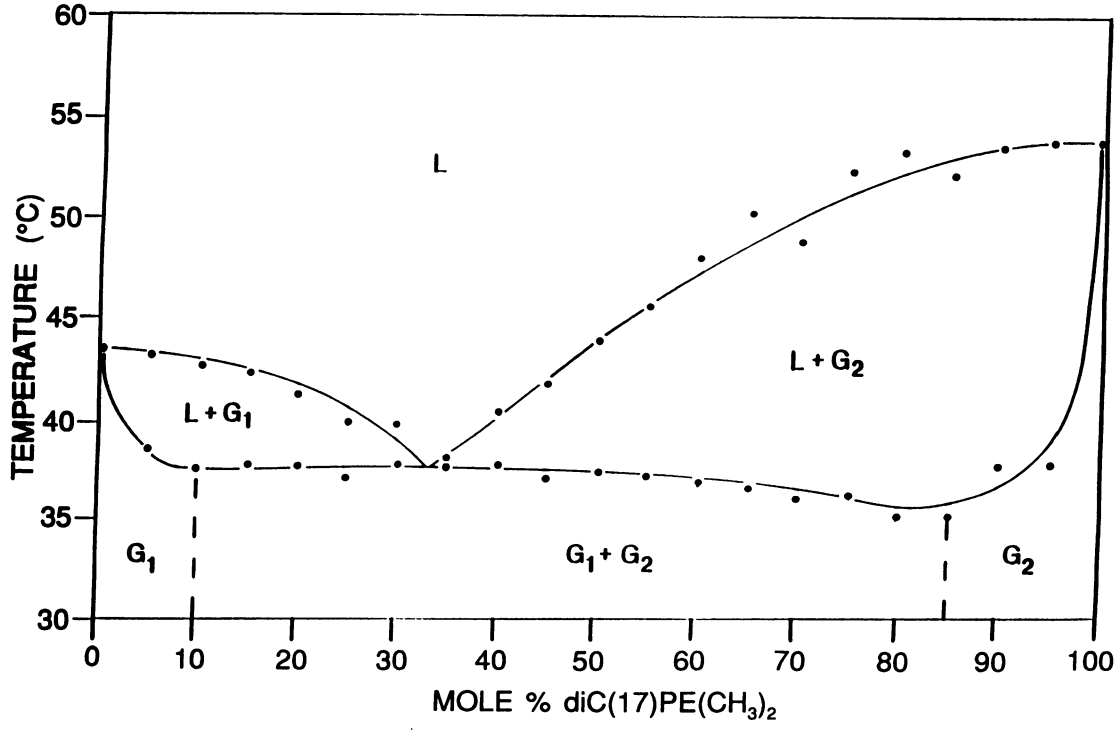

FIGURE 3 The temperature-composition phase diagram for C(22):C(12)PC/C(17):C(17)PE$(CH_3)_2$ mixtures. The solid lines representing the solidus and liquidus phase boundaries are drawn by hand to fit the onset and completion temperatures, respectively, of the transition curves for the various mixtures after correction for the finite width of the two pure component transition curves. The dotted vertical lines represent the solvus lines corresponding approximately to the two ends of the eutectic horizontal.

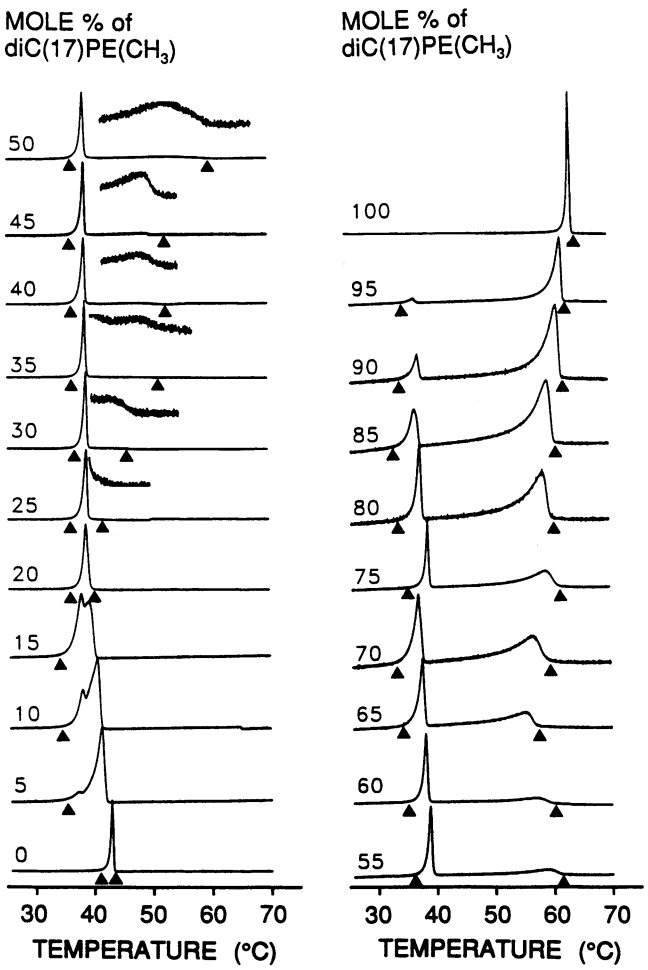

FIGURE 4 DSC heating thermograms for aqueous dispersions of C(22):C(12)PC containing various amounts of C(17):C(17)PE(CH_3). The mole percent of C(17):C(17)PE(CH_3) in each of the binary mixtures is indicated adjacent to the respective thermogram. The onset and completion temperatures of the main transitions are indicated by the triangles.

the mole percent of *N*-methyl-C(17):C(17)PE increases, the transition temperature of the mixture decreases from 43.1 ± 0.5°C (100 mol % C(22):C(12)PC) to 38.0 ± 0.5°C (15 mol percent *N*-methyl-C(17):C(17)PE) and then increases continuously to 63.6 ± 0.25°C (100 mol percent *N*-methyl-C(17):C(17)PE). Like the transitions shown in Fig. 2, the single transition DSC curves shown in Fig. 4 broaden with the incorporation of 5 mol % *N*-methyl-C(17):C(17)PE. These, then, progressively narrow with further increases in *N*-methyl-C(17):C(17)PE content to ~20 mol %. At 20 mol % *N*-methyl-C(17):C(17)PE, the transition curve is the sharpest of any obtained for the C(22):C(12)PC/*N*-methyl-C(17):C(17)PE mixtures. Above 20 mol % *N*-methyl-C(17):C(17)PE, the transition curves steadily broaden to ~95 mol % *N*-methyl-C(17):C(17)PE.

Onset and completion temperatures of the various thermograms, indicated by the triangles in Fig. 4, were used to construct the temperature-composition phase diagram shown in Fig. 5. This phase diagram is characteristic of a eutectic system and similar to the phase diagrams for the C(22):C(12)PC/C(17):C(17)PC and C(22):C(12)PC/*N*,*N*-dimethyl-C-(17):C(17)PE mixtures, with respect to the eutectic horizontal temperature (Fig. 3). In Fig. 5 the eutectic horizontal is located at a temperature of ~37.7 ± 0.5°C and spans the range from 5 to 90 mol % *N*-methyl-C(17):C(17)PE. The eutectic point is located at ~18 mol % *N*-methyl-C(17):C(17)PE and 37.7 ± 0.5°C.

Binary mixtures of C(22):C(12)PC/C(17):C(17)PE

The final set of binary mixtures in this series is composed of C(22):C(12)PC and C(17):C(17)PE. DSC scans of hydrated, pure C(17):C(17)PE aqueous dispersions display a single transition with a T_m of 68.2 ± 0.25°C and a ΔH of 5.3 kcal/mol (Fig. 1 *D*). These values for the lamellar gel/liquid-crystalline phase transition agree with those reported by Lewis et al. (Lewis et al., 1986). Fig. 6 depicts typical DSC heating thermograms for aqueous dispersions of C(22):C(12)PC/C(17):C(17)PE binary mixtures. These thermograms represent the third DSC heating scans for each sample. All samples were scanned over the temperature range of 25–75°C. As the mol percent of C(17):C(17)PE increases, the transition temperature of the mixture decreases from 43.1 ± 0.5°C (100 mol % C(22):C(12)PC) to 38 ± 0.5°C (10 mol % C(17):C(17)PE) and then increases continuously to 68.2 ± 0.25°C (100 mol percent C(17):C(17)PE). Like the transitions shown in Figs. 2 and 4, the single transition DSC curves shown in Fig. 6 quickly broaden with the incorporation of 5 mol % C(17):C(17)PE and then progressively narrow as the C(17):C(17)PE content increases to ~10–15 mol %. At 15 mol % C(17):C(17)PE the transition is the sharpest of any obtained for the C(22):C(12)PC/C(17):C(17)PE mixtures. Above 15 mol % C(17):C(17)PE, the transition curves gradually broaden to ~95 mol % C(17):C(17)PE.

Onset and completion temperatures of the various thermograms, indicated by the triangles in Fig. 6, were used to construct the temperature-composition phase diagram shown in Fig. 7. Like the phase diagram for C(22):C(12)PC/C(17):C(17)PC, C(22):C(12)PC/*N*,*N*-dimethyl-C(17):C(17)PE, and C(22):C(12)PC/*N*-methyl-C(17):C(17)PE mixtures (Figs. 3 and 5), this phase diagram is characteristic of a eutectic system and similar, with respect to the eutectic horizontal temperature. In

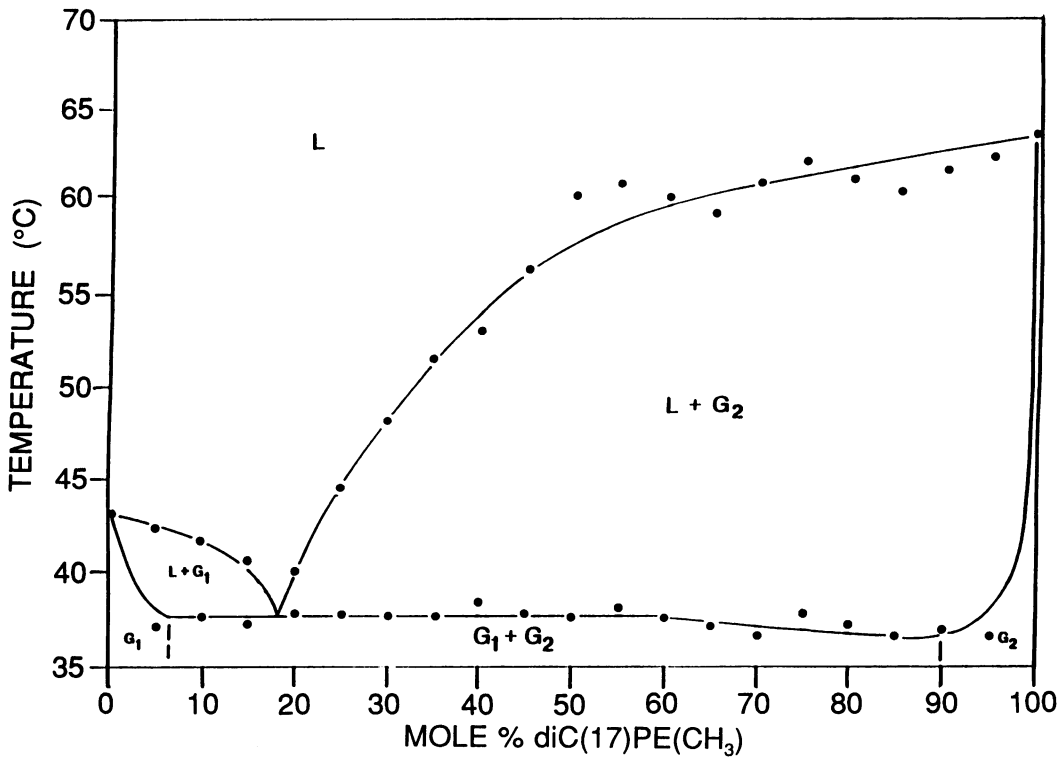

FIGURE 5 The temperature-composition phase diagram for C(22):C(12)PC/C(17):C(17)PE(CH_3) mixtures. The solid lines representing the solidus and liquidus phase boundaries are drawn by hand to fit the onset and completion temperatures, respectively, of the transition curves for the various mixtures after correction for the finite width of the two pure component transition curves. The dotted vertical lines represent the solvus lines corresponding approximately to the two ends of the eutectic horizontal.

Fig. 7 the eutectic horizontal is located at a temperature of ~38.0 ± 0.5°C and spans the range from 4 to 95 mol % C(17):C(17)PE. The eutectic point is located at ~12 mol % C(17):C(17)PE and 38.0 ± 0.5°C.

DISCUSSION

To evaluate the effect of headgroup–headgroup interactions on lateral phase separation within two component bilayers, we have examined the mixing behavior in a series of binary phospholipid mixtures where the headgroup of one component has been progressively demethylated. Here we present the eutectic phase diagrams for C(22):C(12)PC/*N*,*N*-dimethyl-C(17):C(17)PE, C(22):C(12)PC/*N*-methyl-C(17):C(17)PE, and C(22):C(12)PC/C(17):C(17)PE. Together with the previously reported eutectic phase diagram for C(17):C(17)PC/C(22):C(12)PC (Sisk et al., 1990), we have a series of phase diagrams that depicts the effects of changing headgroup-headgroup interactions on the mixing behavior of phospholipid/phospholipid binary mixtures. Because the acyl chains of the phospholipids constituting the four sets of binary mixtures are identical, the observed differences in the shape of the phase diagrams are a direct result of the progressive demethylation of the C(17):C(17)PC headgroup.

The role of headgroup structure in the formation of gel phases has been extensively studied for dimethyl-PE, monomethyl-PE, and PE (Xu et al., 1988; Silvius et al., 1986; Pascher and Sundell, 1986; Mulukutla and Shipley, 1984; Casal and Mantsch, 1983; and Seddon et al., 1983). When initially heated, aqueous C(17):C(17)-PE(CH_3)$_2$ dispersions display a single highly cooperative endothermic transition at 55.6°C corresponding to the L_β to L_α phase transition (Fig. 1 *B*). DSC heating scans of dimethyl-PE dispersions, unlike those for PC dispersions, do not display a transition corresponding to the metastable $P_{\beta'}$ gel phase. Unless annealed under specific conditions, successive heating scans display only the 55.6°C transition. Initial heating scans of properly annealed dimethyl-PE dispersions display two endothermic transitions that correspond to the L_c to L_β and the L_β to L_α phase transitions (Mulukutla and Shipley, 1984).

Monomethyl-PE dispersions display phase behavior similar to dimethyl-PE dispersions. The unheated sam-

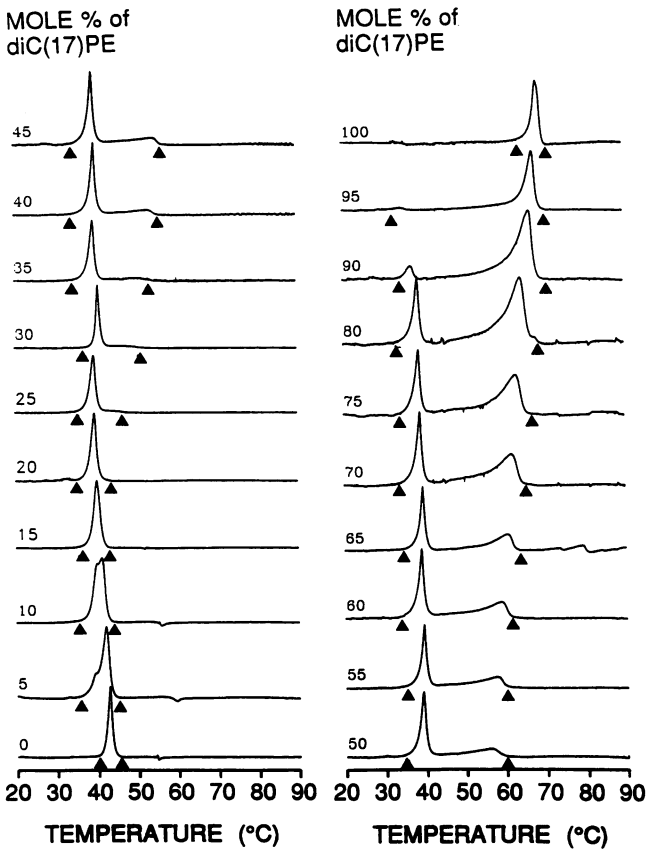

FIGURE 6 DSC heating thermograms for aqueous dispersions of C(22):C(12)PC containing various amounts of C(17):C(17)PE. The mole percent of C(17):C(17)PE in each of the binary mixtures is indicated adjacent to the respective thermogram. The onset and completion temperatures of the main transitions are indicated by the triangles.

ple of C(17):C(17)PE(CH_3) displays a highly cooperative endothermic transition at 63.6°C, corresponding to the L_β to L_α phase transition, that does not shift when cooled to 10°C and immediately rescanned. If annealed under proper conditions, monomethyl-PE dispersions have been shown to form a L_c phase from the L_β gel phase (Mulukutla and Shipley, 1984). When heated, however, the L_c phase does not undergo direct conversion to the L_α phase as demonstrated for PE dispersions, but converts to the L_β gel phase. Thus DSC heating scans of samples that have been annealed under specific conditions display two separate endothermic transitions which correspond to the L_c to L_β and L_β to L_α phase transitions. In the initial and subsequent heating scans, the L_β to L_α phase transition occurs at about the same temperature. The second immediate reheating scan of an annealed monomethyl-PE sample does not display the L_c to L_β phase transition.

Studies of identical-chain PEs indicate that the value of T_m is dependent upon the thermal history of the lipid sample. This temperature dependency is most likely due to the results of the hydrogen bonding and electrostatic interactions between PE headgroups in adjacent bilayers (Xu et al., 1988). Interbilayer hydrogen bonding and electrostatic interactions are most likely to occur between bilayers in the L_c phase in which the interbilayer space is ~5 Å (McIntosh and Simon, 1986). Once a sample is heated above its T_m, the PE headgroup becomes fully hydrated. Upon cooling, the headgroup remains hydrated and the sample forms the L_β gel phase. Only after annealing under specific conditions will the less hydrated L_c phase reform from the fully hydrated L_β gel phase. The first DSC heating scan of pure C(17):C(17)PE in excess water displays a single endothermic transition at 70.9°C with a ΔH of 9.4 kcal/mol corresponding to the L_c to L_α phase transition (Fig. 1 *E*). This value agrees with previously reported values for the first heating scan of a pure C(17):C(17)PE sample (Lewis et al., 1989). The second heating scan of C(17):C(17)PE displays a single endothermic transition at 68.2°C with a ΔH of 5.3 kcal/mol and corresponds to the fully hydrated L_β to L_α phase transition (Fig. 1 *D*). Subsequent DSC scans of this C(17):C(17)PE dispersion display a single endothermic transition, at about the same temperature and about equal in ΔH.

Progressive demethylation of the PC headgroup gradually changes the phospholipids' physical properties from "PC-like" to "PE-like" (Vaughan and Keough, 1974; Casal and Mantsch, 1983; Mulukutla and Shipley, 1984; Gagne et al., 1985; Chowdhry and Dalziel, 1985; Silvius et al., 1986). This gradual change is illustrated by a linear increase in the T_m from 48.8°C for C(17):C(17)PC to 68.2°C for fully hydrated C(17):C(17)PE (Fig. 8 *A*). Both ΔH and ΔS increase with the removal of the first methyl group and then decrease with the removal of each subsequent methyl group (Fig. 8 *B*). Analogous behavior has been shown for both the dimyristoyl and the dipalmitoyl series of identical-chain phospholipids (Mulukutla and Shipley, 1984; Casal and Mantsch, 1983). In addition, it appears that progressive demethylation of the DPPC headgroup increases gel phase bilayer thickness as a result of the decrease in acyl chain tilt (McIntosh, 1980; Simon et al., 1991).

In a previous study we examined the phase behavior of C(22):C(12)PC/C(17):C(17)PC mixtures (Sisk et al., 1990). As a result of the disparity in packing, C(22):C(12)PC/C(17):C(17)PC mixtures are immiscible in the gel phase. C(17):C(17)PC forms a partially interdigitated gel phase bilayer of greater thickness than the mixed interdigitated C(22):C(12)PC gel phase bilayer. Because C(22):C(12)PC and C(17):C(17)PC have identical headgroups, the eutectic phase structure demonstrated for C(22):C(12)PC/C(17):C(17)PC mixtures is

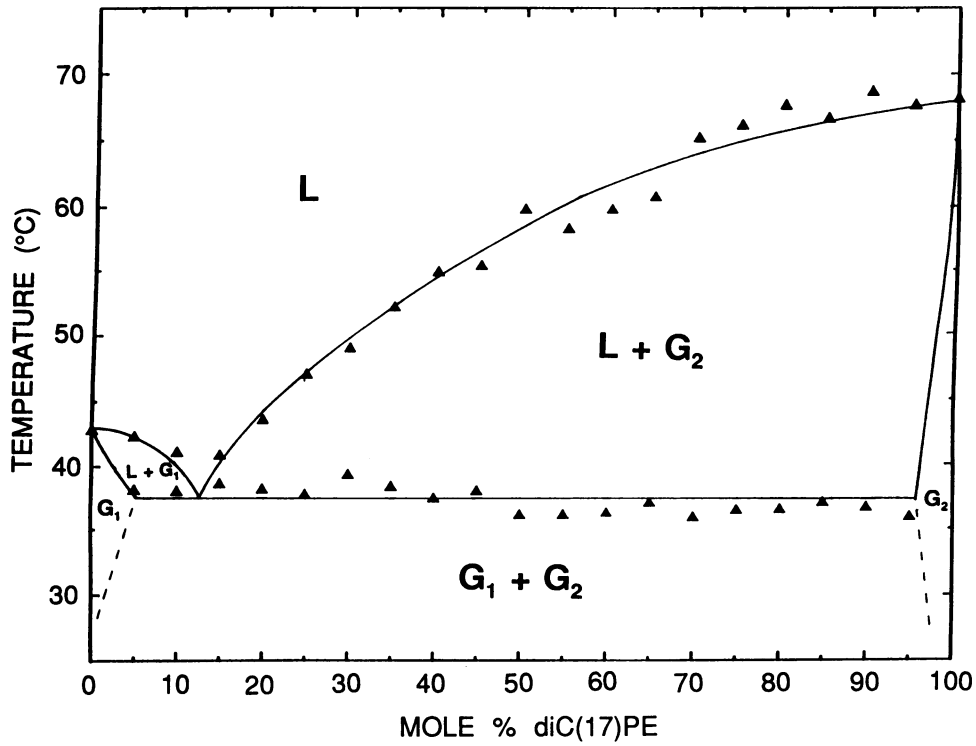

FIGURE 7 The temperature-composition phase diagram for C(22):C(12)PC/C(17):C(17)PE mixtures. The solid lines representing the solidus and liquidus phase boundaries are drawn by hand to fit the onset and completion temperatures, respectively, of the transition curves for the various mixtures after correction for the finite width of the two pure component transition curves. The dotted vertical lines represent the solvus lines corresponding approximately to the two ends of the eutectic horizontal.

dictated by the difference in acyl chain lengths between the two phospholipids.

In the present study, we examined the mixing behavior of C(22):C(12)PC with C(17):C(17)PE$(CH_3)_2$, C(17):C(17)PE(CH_3), or C(17):C(17)PE, a series of phospholipids that have identical length acyl chains but different headgroups. In the gel phase these mixtures display increased lateral phase separation as a result of many factors such as steric crowding, hydrogen bonding interactions, and hydration. As the C(17):C(17)PC headgroup is demethylated, interactions with other C(17):C(17)PXs are favored over interactions with C(22):C(12)PC. With the removal of each methyl group, the likelihood of interaction between C(17):C(17)PX and C(22):C(12)PC decrease in favor of interactions between identical phospholipids. Thus PX–PX pairing becomes increasingly stronger as the PX headgroup is demethylated; lateral phase separation and T_m increase while the eutectic point (triple point) is shifted further to the left in a linear manner (Fig. 9). Each shift represents a decrease in the mole percent of C(17):C(17)PX that comprises the eutectic composition. The increase in immiscibility is reflected by the enlargement of the $L + G_2$ and $G_1 + G_2$ two phase regions; a concomitant decrease in the areas of the $L + G_1$ two phase region, and the G_1 and G_2 one phase regions, are observed.

Differences in van der Waals chain–chain interactions resulting from steric crowding of the C(17):C(17)PX headgroup influence gel phase lateral separation within the C(22):C(12)PC/C(17):C(17)PX bilayer. Headgroup crowding occurs in the C(17):C(17)PC gel phase because the cross-sectional area of the PC headgroup is larger than the overall cross-sectional area occupied by its two acyl chains at $T < T_m$ (McIntosh, 1980; Wilkinson and Nagle, 1981). In a pure component C(17):C(17)PC bilayer, the difference between the cross-sectional area of the headgroup and that of the acyl chains is reduced by the tilting of the acyl chains to fill the void caused by headgroup steric crowding (McIntosh, 1980; Casal and Mantsch, 1983; Simon et al., 1991). In C(22):C(12)PC/C(17):C(17)PC mixtures the two components are separated in the gel phase because C(17):C(17)PC acyl chains pack tilted with respect to the bilayer normal, whereas C(22):C(12)PC acyl chains pack perpendicular to the plane of the bilayer. There are strong van der

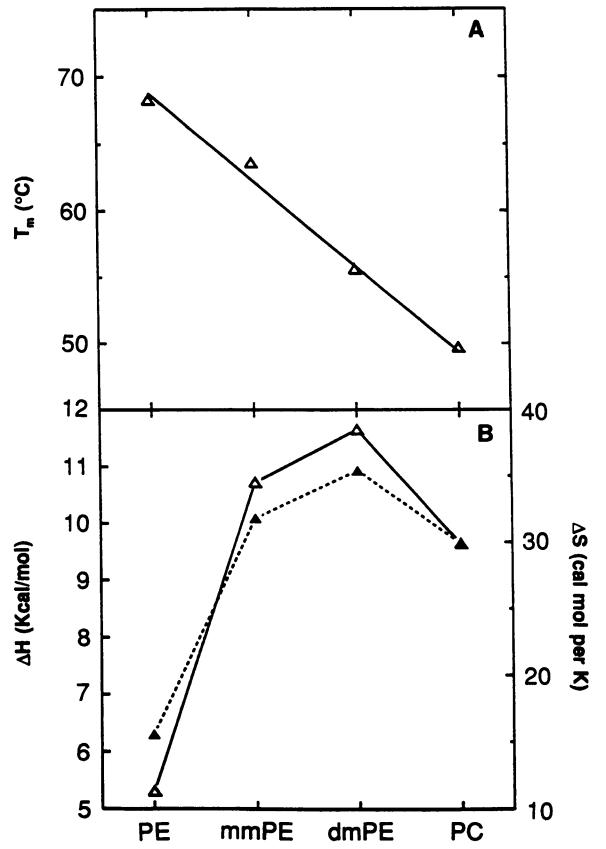

FIGURE 8 The effect of PE methylation on the main transition temperature (*A*) and both the enthalpy (△, *solid line*) and entropy (▲, *dotted line*) (*B*) of C(17):C(17)PX.

Waals interactions between the parallel acyl chains of identical lipids, (i.e., C(22):C(12)PC or C(17):C(17)PC). In contrast, the acyl chains of C(22):C(12)PCs (perpendicular to the bilayer normal) and the acyl chains of C(17):C(17)PCs (tilted with respect to the bilayer normal) do not pack close enough to form strong van der Waals interactions.

In mixtures of C(22):C(12)PC and C(17):C(17)PX, as the C(17):C(17)PC headgroup is progressively demethylated, its cross-sectional area decreases. Subsequently, as the C(17):C(17)PX acyl chains approach 90° to the plane of the bilayer normal, they pack close enough to the acyl chains of C(22):C(12)PC to form van der Waals interactions. However, as the C(17):C(17)PX acyl chains become more parallel to the acyl chains of C(22):C(12)PC, the thickness of the C(17):C(17)PX domain increases to a maximum thickness greater than that of the C(22):C(12)PC domain at $T < T_m$. The resulting difference in the bilayer thickness would cause the hydrophobic C(17):C(17)PX acyl chains to be exposed to the hydrophilic C(22):C(12)PC headgroup and surrounding solvent. Because exposure of the hydrophobic acyl chains to hydrophilic areas is unfavorable energetically, a progressive increase in the lateral separation of C(17):C(17)PX and C(22):C(12)PC in the plane of the bilayer is thus expected.

Because the headgroup of PC is the only phospholipid species in the series of PX that has no H-bond donor, the headgroup–headgroup interactions in the PC/PC mixtures is thus the weakest. PE molecules, on the other hand, can undergo H-bond interactions in PE/PE mix-

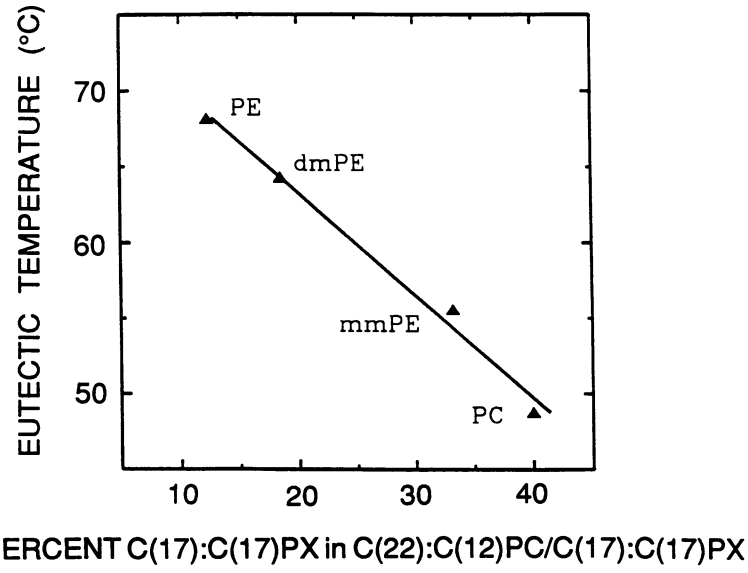

FIGURE 9 The effect of C(17):C(17)PE headgroup methylation on the eutectic composition for the C(22):C(12)PC/C(17):C(17)PX mixtures is plotted against the T_m of C(17):C(17)PX.

tures via their amine moieties in the headgroups. Hence, in the binary mixtures of PE and PC, the PE molecules tend to aggregate together due to their favorable headgroup–headgroup interactions. Similarly PX–PX interactions are stronger than PC–PC interactions. Consequently, in addition to headgroup crowding, hydrogen bonding interactions between identical headgroups may also play an important role in causing increased gel phase immiscibility in C(22):C(12)PC/C(17):C(17)PX mixtures as the C(17):C(17)PX headgroup is progressively demethylated.

While the areas of the phase diagram regions change with progressive demethylation of the PX headgroup, the phase diagram retains its eutectic nature. The onset temperature of the phase transition for binary mixtures defines the solidus line of a eutectic phase diagram. For the mixtures studied here, the onset temperature is determined by the lower melting C(22):C(12)PC component. Addition of either C(17):C(17)PC, C(17):C(17)PE$(CH_3)_2$, C(17):C(17)PE(CH_3), or C(17):C(17)PE to the C(22):C(12)PC bilayer lowers the onset temperature by the same amount, ~5–6°C, for all mixtures that fall on the eutectic horizontal. This is an interesting effect in light of the differences in the transition temperatures of the various C(17):C(17)PX components. Depression of the C(22):C(12)PC onset temperature for acyl chain melting in C(22):C(12)PC/C(17):C(17)PX bilayers suggests that the hydrophobic region of the mixed interdigitated gel phase bilayer can be perturbed by the presence of small amounts of C(17):C(17)PX (G_1 phase). Because the addition of any of the PX components lowers the onset temperature by the same amount, the structural property that determines the onset temperature must be similar in all of the PX phospholipids. Each PX component has a different headgroup but identical acyl chains; therefore, the acyl chain interactions between C(22):C(12)PC and contaminating amounts of C(17):C(17)PX in the G_1 gel phase are independent of the headgroup.

In this study we investigated changes in gel phase miscibility using mixtures of C(22):C(12)PC and progressively demethylated C(17):C(17)PX components. Our results suggest that the eutectic composition is influenced by changes in gel phase acyl chain packing that are dependent on headgroup-headgroup interactions. In contrast, the eutectic nature of the phase diagram and the location of its solidus line are properties of acyl chain interactions that are independent of phospholipid headgroup–headgroup interactions.

This research was supported in part by United States Public Health Service Grant GM-17452 from the National Institute of General Medical Sciences, National Institutes of Health, Department of Health and Human Services.

Received for publication 9 September 1991 and in final form 14 November 1991.

REFERENCES

Bultmann, T., H-n. Lin, Z-q. Wang, and C. Huang. 1991. Thermotropic and mixing behavior of mixed-chain phosphatidylcholines with molecular weights identical with that of L-α-Dipalmitoylphosphatidylcholine. *Biochemistry.* 30:7194–7202.

Casal, H. L., and H. H. Mantsch. 1983. The thermotropic behavior of *n*-methylated dipalmitoylphosphatidylethanolamines. *Biochim. Biophys. Acta.* 735:387–396.

Chowdhry, B. Z., and A. W. Dalziel. 1985. Phase transitions properties of 1,2 and 1,3-diacylphosphatidylethanolamines with modified head groups. *Biochemistry.* 24:4109–4117.

Comfurius, P. and R. F. A. Zwaal. 1977. The enzymatic synthesis of phosphatidylserine and purification by CM-cellulose column chromatography. *Biochim. Biophys. Acta.* 488:36–42.

Gagne, J., L. Stamatatos, T. Diacovo, S. W. Hui, P. L. Yeagle, and J. R. Silvius. 1985. Physical properties and surface interactions of bilayer membranes containing *n*-methylated phosphatidylethanolamines. *Biochemistry* 24:4400–4408.

Gardam, M., and J. R. Silvius. 1989. Intermixing of dipalmitoylphosphatidylcholine with phospho and sphingolipids bearing highly asymmetric hydrocarbon chains. *Biochim. Biophys. Acta.* 980:319–325.

Huang, C. 1990. Mixed-chain phospholipids and interdigitated bilayer systems. *Klin. Wochenschr.* 68:149–165.

Huang, C. 1991. Empirical estimation of the gel to liquid-crystalline phase transition temperatures for fully hydrated saturated phosphatidylcholines. *Biochemistry.* 30:26–30.

Hui, S. W., J. T. Mason, and C. Huang. 1984. Acyl chain interdigitation in saturated mixed-chain phosphatidylcholine bilayer dispersions. *Biochemistry.* 23:5570–5577.

Lewis, R. N. A., D. A. Mannock, and R. N. McElhaney. 1989. Effect of fatty acyl chain length and structure on the lamellar gel to liquid-crystalline and lamellar to reversed hexagonal phase transitions of aqueous phosphatidylethanolamine dispersions. *Biochemistry.* 28: 541–548.

Lin, H-n., Z-q. Wang, and C. Huang. 1991. The influence of acyl chain-length asymmetry on the phase transition parameters of phosphatidylcholine dispersions. *Biochim. Biophys. Acta.* 1067:17–28.

Lin, H-n., Z-q. Wang, and C. Huang. 1990. Differential scanning calorimetry study of mixed-chain phosphatidylcholines with a common molecular weight identical with diheptadecanoylphosphatidylcholine. *Biochemistry.* 29:7063–7072.

Lin, H-n., and C. Huang. 1988. Eutectic phase behavior of 1-stearoyl-2-caprylphosphatidylcholine and dimyristoylphosphatidylcholine mixtures. *Biochim. Biophys. Acta.* 946:178–184.

Mabrey, S., and J. M. Sturtevant. 1976. Investigation of phase transitions of lipids and lipid mixtures by high sensitivity differential scanning calorimetry. *Proc. Natl. Acad. Sci. USA.* 73:3862–3866.

Mason, J. T., A. V. Broccoli, and C. Huang. 1981a. A method for the synthesis of isomerically pure saturated mixed-chain phosphatidylcholines. *Anal. Biochem.* 113:96–101.

Mason, J. T., C. Huang, and R. L. Biltonen. 1981b. Calorimetric investigations of saturated mixed-chain phosphatidylcholine bilayer dispersions. *Biochemistry.* 20:6086–6092.

Mattai, J., P. K. Sripada, and G. G. Shipley. 1987. Mixed-chain phosphatidylcholine bilayers: structure and properties. *Biochemistry.* 26:3287–3297.

McIntosh, T. J. 1980. Differences in hydrocarbon chain tilt between hydrated phosphatidylethanolamine and phosphatidylcholine bilayers. *Biophys. J.* 29:237–246.

McIntosh, T. J., and S. A. Simon. 1986. Area per molecule and distribution of water in fully hydrated dilauroylphosphatidylethanolamine bilayers. *Biochemistry.* 25:4948–4952.

McIntosh, T. J., S. A. Simon, J. C. Ellington, Jr., and N. A. Porter. 1984. New structural model for mixed-chain phosphatidylcholine bilayers. *Biochemistry.* 23:4038–4044.

Mulukutla, S., and G. G. Shipley. 1984. Structure and Thermotropic Properties of Phosphatidylethanolamine and its n-methyl derivatives. *Biochemistry.* 23:2514–2519.

Pascher, I. and S. Sundell. 1986. Membrane lipids: preferred conformational states and their interplay. The crystal structure of dilauroylphosphatidyl-*N*,M-dimethylethanolamine. *Biochim. Biophys. Acta.* 855:68–78.

Perrin, D. D., and W. L. F. Armarego. 1988. Purification of laboratory chemicals. Third edition. Pergamon Press Inc., New York.

Seddon, J. M., K. Harlos, and D. Marsh. 1983. Metastability and polymorphism in the gel and fluid bilayer phases of dilauroylphosphatidylethanolamine. *J. Biol. Chem.* 258:3850–3854.

Shah, J., P. K. Sripada, and G. G. Shipley. 1990. Structure and properties of mixed-chain phosphatidylcholine bilayers. *Biochemistry.* 29:4254–4262.

Silvius, J. R., 1986. Solid- and liquid-phase equilibria in phosphatidylcholine/phosphatidylethanolamine mixtures. A calorimetric study. *Biochim. Biophys. Acta.* 857:217–228.

Silvius, J. R., P. M. Brown, and T. J. O'Leary. 1986. Role of head group structure in the phase behavior of amino phospholipids. 1. Hydrated and dehydrated lamellar phases of saturated phosphatidylethanolamine analogues. *Biochemistry.* 25:4249–4258.

Simon, S. A., C. A. Fink, A. K. Kenworthy, and T. J. McIntosh. 1991. The hydration pressure between lipid bilayers. Comparison of measurements using x-ray diffraction and calorimetry. *Biophys. J.* 59:538–546.

Sisk, R. B., Z-q. Wang, H-n. Lin, and C. Huang. 1990. Mixing behavior of identical molecular weight phosphatidylcholines with various chain-length differences in two-component lamellae. *Biophys. J.* 58:777–783.

Slater, J. L., and C. Huang. 1988. Interdigitated bilayer membranes. *Prog. Lipid Res.* 27:325–359.

Vaughan, D. J., and K. M. Keough. 1974. Changes in phase transitions of phosphatidylethanolamine- and phosphatidylcholine-water dispersions induced by small modifications in the headgroup and backbone regions. *FEBS (Fed. Eur. Biochem. Soc.) Lett.* 47:158–161.

Wilkinson, D. A., and J. F. Nagle. 1981. Dilatometry and calorimetry of saturated phosphatidylethanolamine dispersions. *Biochemistry.* 20:187–192.

Xu, H., F. A. Stephenson, H. Lin, and C. Huang. 1988. Phase metastability and supercooled metastable state of diundecanoylphosphatidylethanolamine bilayers. *Biochim. Biophys. Acta.* 943:63–75.

Yeagle, P. 1987. The Membranes of Cells. Academic Press, Inc., New York.